Supplementary Information

Thermodynamic Properties of Lower Critical Solution Temperature (LCST) Mixtures and Their Application in Energy-Water Systems

Jordan D. Kocher[a], Ahmed Mahfouz[a], Jesse G. McDaniel[b], and Akanksha K. Menon[a*]

[a]George W. Woodruff School of Mechanical Engineering, Georgia Institute of Technology, Atlanta, GA, USA

[b]School of Chemistry and Biochemistry, Georgia Institute of Technology, Atlanta, GA 30332, USA

*Corresponding author. Email: akanksha.menon@me.gatech.edu

Supplementary Note 1: Water Activity and Mass Fraction Measurements of Oleic Acid/Lidocaine (OA/LD) and $P_{4444}TFA$ (PTFA)

We measured the water activity of aqueous mixtures of PTFA[1–3] and OA/LD[4,5] at 25 °C as a function of the mass fraction of the LCST species (PTFA and OA/LD, respectively). The water activity data was used to generate the chemical potential of water plots in Fig. S1a and Fig. S1b. By numerically integrating Eq. (8) of the main text, we also generated the chemical potential of PTFA, shown in Fig. S1c. The same plot cannot be generated for OA/LD since that is a ternary mixture (oleic acid + lidocaine + water), so Eq. 8 of the main text does not apply, and we have no way of directly measuring the oleic acid or lidocaine chemical potential. For PTFA, activity measurements from our prior work[6] are used for mass fractions from 10 to 70 wt%, while we took new measurements for 80 and 90 wt%. Each data point in Fig. S1 represents the average of five water activity measurements.

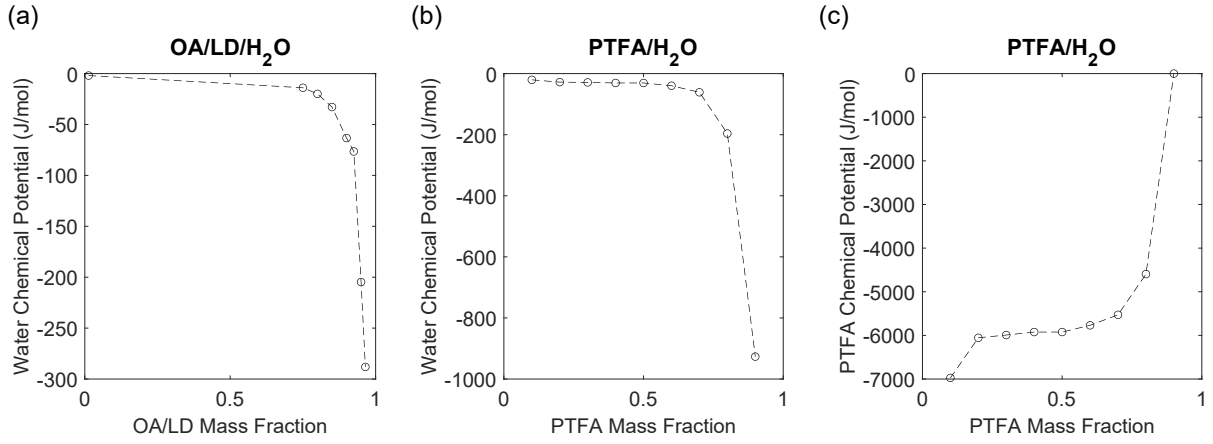

Fig. S1. Chemical potential of different species in LCST mixtures at 25 °C. (a) Chemical potential of water in OA/LD/H_2O. (b) Chemical potential of water in PTFA/H_2O. (c) Chemical potential of PTFA in PTFA/H_2O.

In this work, we consider the "ideal" LCST mixture to be one with a water-rich (WR) phase that is pure water, with a water activity of unity. The chemical potential of water in this ideal WR

phase would not change as a function of temperature (since it is pure water, which has zero chemical potential of water at any temperature). Then, in the ideal case, all of the chemical potential change required for the WR and WS concentrations to have equal chemical potentials of water at the separation temperature (T_2 in the main text) would come from the WS phase ($\Delta\mu_q$ in the main text). We used the fact that the chemical potential of water changes as a function of temperature for the WS phase only (in the ideal case) to derive the partial molar enthalpy and entropy under certain conditions in the main text.

In the main text, we mentioned that chemical potential of both species must be monotonic at temperatures below the LCST. This is the case for the water chemical potential in OA/LD and PTFA at 25 °C, as shown in Fig. S1a and b. We note that a slight variation in water activity at 30 wt% PTFA led to a larger jump in Fig. S1c at the same weight percent – this is simply an artefact of the integration used to construct Fig. S1c from Fig. S1b, which was generated from the measured water activity values.

To see how closely real LCST mixtures conform to this ideal case, we measured the chemical potential of water in the WR and WS phases of PTFA/H_2O and OA/LD/H_2O as a function of temperature, which is presented in Fig. S2. For PTFA, we used the phase diagram to determine the WR and WS concentrations (15 and 63 wt% PTFA, respectively). We then prepared mixtures of these concentrations and measured their activities as a function of temperature; this data is presented in Fig. S2a. However, the phase diagram of OA/LD has not been reported in literature, so we have no reference to determine the concentrations of the WR and WS phases. Instead, we prepared two OA/LD mixtures, each with 25 wt% OA, 25 wt% LD, and 50 wt% water. The first OA/LD sample was heated to 35 °C and the two phases were separated, while the second was heated to 70 °C and then separated.

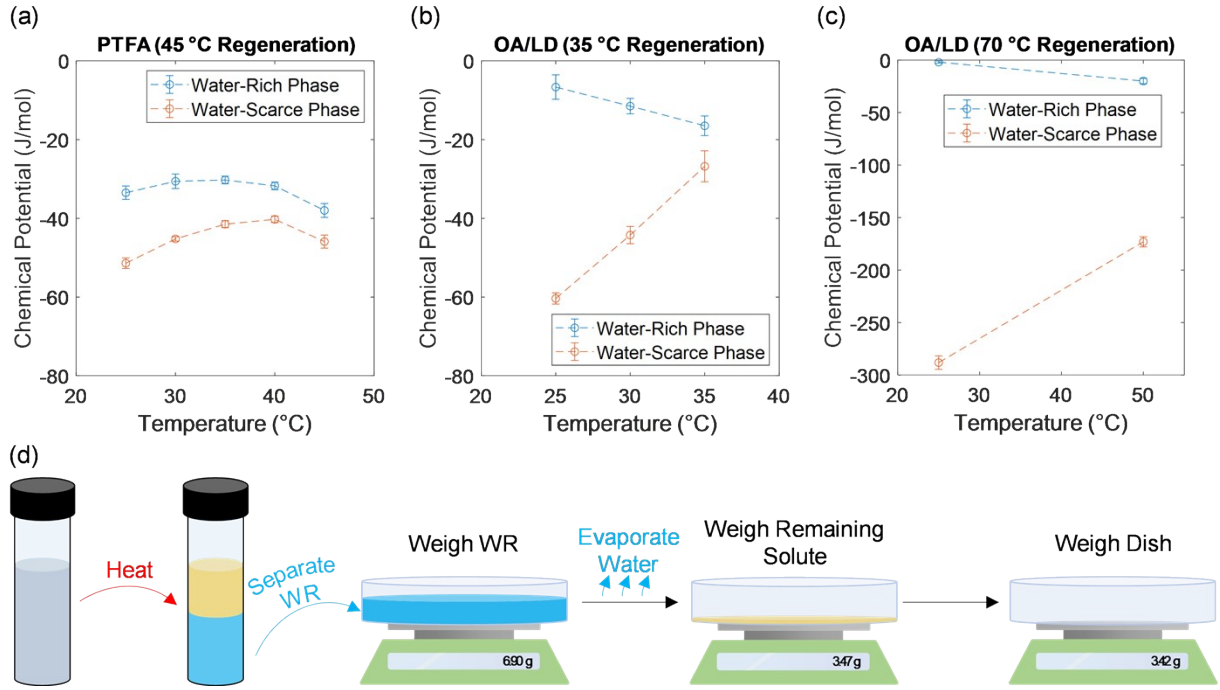

Fig. S2. Characterization of PTFA and OA/LD mixtures after phase separation. (a) Chemical potential of water in the water-rich (WR) and water-scarce (WS) phases of aqueous PTFA corresponding to 45 °C phase separation. (b) Chemical potential of the WR and WS phases of aqueous OA/LD after it was heated up to 35 °C and phase separated. (c) Chemical potential of the WR and WS phases of aqueous OA/LD after it was heated up to 70 °C and phase separated. In (a) – (c), the chemical potential is given as a function of temperature, with the chemical potential of the two phases converging as temperature increases. (d) The process of determining the mass fraction of OA/LD in a particular phase of the phase separated OA/LD/H_2O mixture. The illustration in (d) depicts the mass fraction of the WR phase being measured, but the process was also performed for the WS phase. This was done for the OA/LD mixture that was phase separated at 35 °C and for the one separated at 70 °C. Separation was performed by placing each sample in a water bath for 48 hours. The two phases were then manually separated with a pipette. To determine the mass fraction, water was evaporated from each sample by placing the samples in an environmental chamber set to 50 °C and 0% RH for 24 hours.

The chemical potential of water in the two phases of PTFA in Fig. S2a do not converge at 45 °C, despite the fact that they are in equilibrium at that temperature and therefore must have the same chemical potential. This is likely due to the measurement limit associated with the activity meter; the accuracy listed for the Aqualab 4TE water activity meter is ±0.003, and the activity of the two concentrations are within 0.006 of each other at every temperature other than 25 °C in Fig.

S2a. The chemical potential of the OA/LD sample in Fig. S2b also did not converge at the temperature to which they had been heated and separated. This could have arisen from several experimental factors: (i) imperfect separation when the two phases were manually separated with a pipette (some of the WR phase could have been extracted along with the WS phase, and vice versa), (ii) some of the water could have evaporated from the samples as they were being pipetted into the sample cup and placed into the activity meter, or (iii) activity sensor accuracy limit at higher temperatures. Meanwhile, the activity meter only goes up to 50 °C, so the convergence of the two phases could not be completely measured for the OA/LD sample regenerated at 70 °C (Fig. S2a and Fig. S2c).

Fig. S2 indicates that the behavior of OA/LD is much closer to the "ideal" LCST mixture behavior than PTFA is. Logically, it is intuitive that the chemical potential of the WR phase of PTFA changes more than OA/LD as a function of temperature, since the WR phase of PTFA is about 90 wt% water (according to existing phase diagrams[1]), whereas the WR phase of OA/LD is between 98 wt% and 99 wt% water when regenerated at 70 °C (according to our data, which is presented in Table S1 below). Therefore, the WR phase of OA/LD is closer to the ideal case described in this work than the WR phase of PTFA.

Compared to the OA/LD/H_2O mixture that was heated to 70 °C, the 35 °C heating of OA/LD/H_2O yielded a WR phase with a slightly lower chemical potential and a WS phase with a higher chemical potential. As such, we wanted to measure the mass fraction of water in both phases for both separation temperatures, to confirm that the WR mass fraction of water was higher in the 70 °C case than in the 35 °C case, and the WS mass fraction of water was lower in the 70 °C than in the 35 °C case. Fig. S2d illustrates the method used to determine these mass fractions, and the results are summarized in Table S1.

Table S1. Mass fraction of water in OA/LD/H_2O water-rich and water-scarce phases after being placed in a water bath for 48 hours (to induce phase separation) at different temperatures.

Water Bath Temperature (°C)	Water-Rich Phase Mass Fraction of Water	Water-Scarce Phase Mass Fraction of Water
35	0.981	0.07
70	0.987	0.035

These mass fraction measurements are consistent with our water activity measurements, which show that the water activity of the WR phase is higher when heated at 70 °C than at 35 °C (indicating a higher mass fraction of water in the WR phase with 70 °C heating), while the water activity of the WS phase is lower when heated at 70 °C than at 35 °C (indicating a lower mass fraction of water in the WS with 70 °C heating). Furthermore, while we have not yet measured the LCST phase diagram for OA/LD/H_2O, we have observed that an OA/LD/H_2O mixture with 5 wt% water does phase separate when heated to 70 °C, indicating that the WS phase of OA/LD/H_2O should be less than 5 wt% water at 70 °C, which is again consistent with our measurement of 3.5 wt% water in the WS for 70 °C heating.

In Table 1 of the main text, we provide values for the activity and chemical potential of the WS phase of OA/LD/H_2O and of PTFA/H_2O after phase separation at 323 K. To determine this, we prepared one mixture of PTFA/H_2O (50 wt% PTFA and 50 wt% H_2O), as well as an OA/LD/H_2O mixture (25 wt% OA, 25 wt% LD, 50 wt% H_2O). We then heated the mixtures in a water bath set to 70 °C, separated the phases of each mixture with a pipette, and measured the water activities at ambient temperature (~ 300 K). For PTFA, we measured a water activity of 0.976, whereas for OA/LD, we measured a water activity of 0.890. Our PTFA measurement is in agreement with the data gathered by Kamio *et al*.,[3] while our OA/LD measurement is in agreement with measurements previous measurements that we have reported.[5]

Supplementary Note 2: Derivation of Eq. (11) and (15) from the Main Text

This supplementary note contains the derivation of solution thermodynamic relations that are available in standard textbooks and included here for convenience[7,8]. Applying the appropriate Legendre transformation to the fundamental thermodynamic relation, we get the following relation for a binary mixture:

$$dG = VdP - SdT + \mu_1 dn_1 + \mu_2 dn_2 \tag{S1}$$

And, for a binary mixture, the total differential of G is:

$$dG = \left(\frac{\partial G}{\partial P}\right)_{T,n_1,n_2} dP + \left(\frac{\partial G}{\partial T}\right)_{P,n_1,n_2} dT + \left(\frac{\partial G}{\partial n_1}\right)_{T,P,n_2} dn_1 + \left(\frac{\partial G}{\partial n_2}\right)_{T,P,n_1} dn_2 \tag{S2}$$

Thus:

$$\left(\frac{\partial G}{\partial T}\right)_{P,n_1,n_2} = -S \tag{S3}$$

$$\left(\frac{\partial G}{\partial n_1}\right)_{T,P,n_2} = \mu_1 \tag{S4}$$

Since dG is a total differential, the mixed second-order partial derivatives are independent of the order in which they are evaluated:

$$\left(\frac{\partial G}{\partial T \partial n_1}\right)_{P,n_2} = \frac{\partial}{\partial n_1}\left(\left(\frac{\partial G}{\partial T}\right)_{P,n_1,n_2}\right)_{T,P,n_2} = \frac{\partial}{\partial T}\left(\left(\frac{\partial G}{\partial n_1}\right)_{T,P,n_2}\right)_{P,n_1,n_2} \tag{S5}$$

Based on the first expression for dG, we get:

$$\frac{\partial}{\partial n_1}(-S)_{T,P,n_2} = \frac{\partial}{\partial T}(\mu_1)_{P,n_1,n_2} \tag{S6}$$

The partial derivative $\frac{\partial}{\partial n_1}(-S)_{T,P,n_2}$ is equal to the partial molar entropy of species 1 in the mixture ($\bar{s}_1$), such that:

$$\left(\frac{\partial \mu_1}{\partial T}\right)_{P,n_1,n_2} = -\bar{s}_i \tag{S7}$$

A similar approach can be used for species 2. Thus, for a mixture maintained at constant pressure (fixed P) and concentration (fixed n_1 and n_2), the change in chemical potential with respect to temperature is related to the partial molar entropy in the following way (which is identical to Eq. (11) from the main text when species *i* is water):

$$\frac{\partial \mu_i}{\partial T} = -\bar{s}_i \tag{S8}$$

Next, we can rewrite the partial derivative of chemical potential with respect to temperature in the following way:

$$\frac{\partial \mu_i}{\partial T} = \frac{\partial}{\partial T}(\bar{h}_i - T\bar{s}_i) = \frac{\partial \bar{h}_i}{\partial T} - T\frac{\partial \bar{s}_i}{\partial T} - \bar{s}_i \tag{S9}$$

However, from Eq. (S8), we know that $\frac{\partial \mu_i}{\partial T} = -\bar{s}_i$, yielding the following equation (which is identical to Eq. (14) from the main text when species *i* is water):

$$\frac{\partial \bar{h}_i}{\partial T} = T\frac{\partial \bar{s}_i}{\partial T} \tag{S10}$$

Eq. (S10) reveals that the partial molar enthalpy and entropy are inextricably linked as a function of temperature (when concentration and pressure are fixed), so that when one changes, the other changes accordingly. Additionally, if either partial molar enthalpy or entropy is known as a

function of temperature (at some concentration and pressure), the other can be found (at the same concentration and pressure).

Supplementary Note 3: Common Tangent Method

This supplementary note covers a standardized thermodynamic derivation of the common tangent method[7]. In the main text, we discuss the common tangent method of constructing the phase diagram of a thermally responsive mixture. In this section, we give further detail as to why the common tangent coincides with the two concentrations that yield the lowest free energy of the mixture. Fig. S3a shows the molar free energy of mixing at a temperature below the LCST (T_1) and a temperature above the LCST (T_2) – Fig. S3a is identical to Fig. 1b in the main text. In Fig. S3a, the dashed line connecting g_{mix} at x_p and x_q must be tangent to g_{mix} at both x_p and x_q. If it were not tangent, there would exist different concentrations for the two phases that would produce a lower free energy. This is illustrated in Fig. S3b, which shows a zoomed-in view of the g_{mix} curve for $T = T_2$. The tangent connecting g_{mix} at x_p and x_q is drawn as a dashed line, while a line intersecting g_{mix} at two arbitrary concentrations not equal to x_p and x_q is drawn as a dotted line. At any concentration between x_p and x_q, the single-phase state would have the highest free energy. The two-phase state consisting of concentrations not equal to x_p and x_q (*i.e.*, the dotted line) would have a lower free energy than the single-phase state, but a higher free energy than the two-phase state corresponding to x_p and x_q (*i.e.*, the dashed line). Thus, for any concentration between x_p and x_q, the common tangent lies below all lines drawn between any two other points on g_{mix}. Therefore, at T_2, a mixture of any concentration between x_p and x_q would spontaneously separate into a biphasic mixture of x_p and x_q, which are the two points on the binodal curve at T_2.

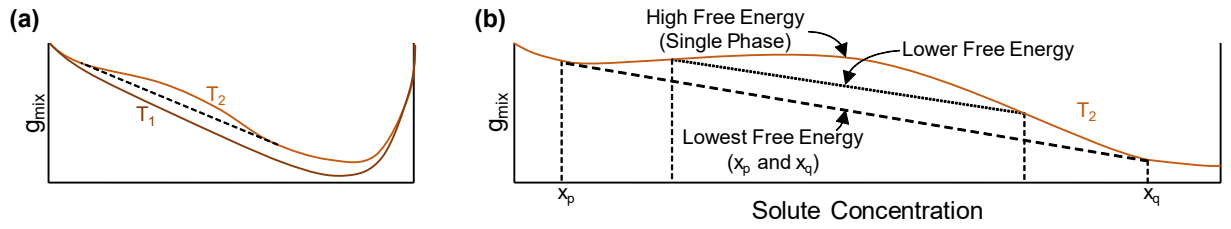

Fig. S3. Common tangent method. (a) Molar free energy of mixing. (b) Zoomed-in portion of (a).

Supplementary Note 4: Materials Synthesis and Preparation

To apply our analysis to real LCST mixtures, we performed water activity measurements on two LCST mixtures: PTFA/H_2O and OA/LD/H_2O. The PTFA was synthesized according to the procedure described by Haddad *et al.*[1] Preparing the OA/LD required no chemical synthesis, since oleic acid and lidocaine can be purchased off-the-shelf from various suppliers. We purchased oleic acid from Lab Alley (C5820-500ml) and lidocaine from Tokyo Chemical Industry (L0156-500G).

Supplementary Note 5: LCST Behavior and Negative Partial Molar Entropy with Positive Entropy of Mixing

LCST phase behavior is often associated with a negative entropy of mixing; however, in this section, we show that this is not a strict requirement and that a positive entropy of mixing could yield LCST behavior. To do this, we utilize Eq. (S11) to model a binary mixture with a non-ideal entropy of mixing, as well as Eq. (S12) to model the non-ideal enthalpy of mixing.

$$s_{mix} = -R\left[x_1 \ln\left(x_1\right) + x_2 \ln\left(x_2\right) + x_1 x_2 \chi_s\right] \quad \text{(S11)}$$

$$h_{mix} = R x_1 x_2 \chi_h \quad \text{(S12)}$$

Using $\chi_s =$ 16 and $\chi_h =$ -4800, we plot the entropy of mixing, enthalpy of mixing, chemical potential, and free energy of mixing in Fig. S4. This negative entropy of mixing yields LCST behavior when the mixture temperature is increased from 300 to 350 K; the existing of a miscibility gap at 350 K is evidenced by the existence of a common tangent on the 350 K curve in Fig. S4d. This is representative of the general behavior that is commonly attributed to LCST mixtures.

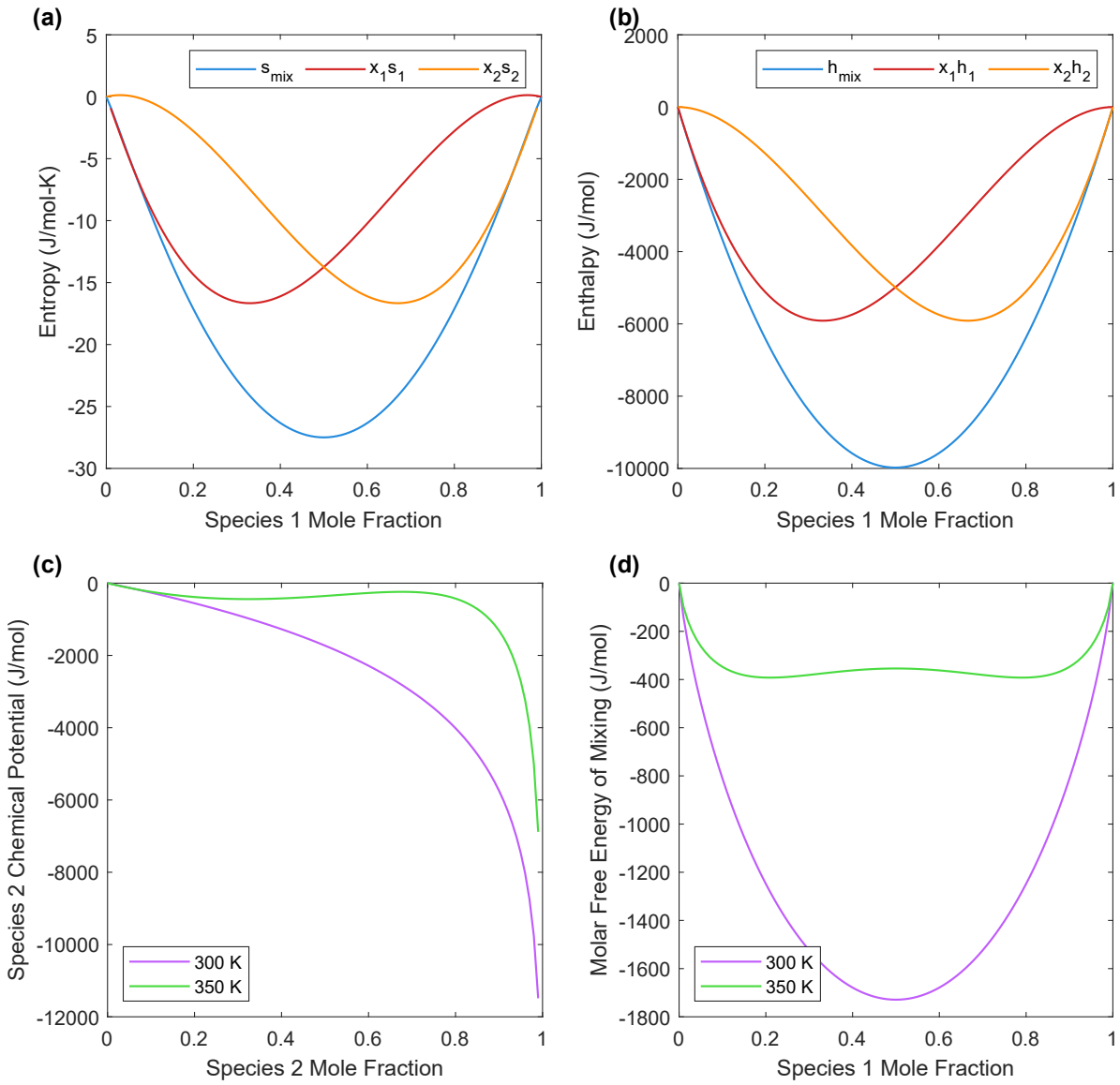

Fig. S4. LCST behavior in a modeled binary mixture with a negative entropy of mixing. (a) Entropy of mixing and partial molar entropies of both species. (b) Enthalpy of mixing and partial molar entropies of both species. (c) Chemical potential at a temperature below the LCST (300 K) and above the LCST (350 K). (d) Free energy of mixing at a temperature below the LCST (300 K) and above the LCST (350 K).

Next, we use $\chi_s =$ 2.7 and $\chi_h =$ -212 to investigate a positive entropy of mixing. We plot the entropy, enthalpy, chemical potential, and free energy associated with these mixing parameters in Fig. S5. In this scenario, the entropy of mixing remains positive at all concentrations. Despite this, the partial molar entropies are negative for a portion of the plot in Fig. S5a. Because of the

negative partial molar entropy, the chemical potentials in both Fig. S4c and Fig. S5c increase with temperature at higher concentrations (though the magnitudes are very different). Furthermore, the existence of a common tangent in Fig. S5d signifies that a miscibility gap exists at 350 K. Thus, LCST behavior is not predicated upon a negative entropy of mixing.

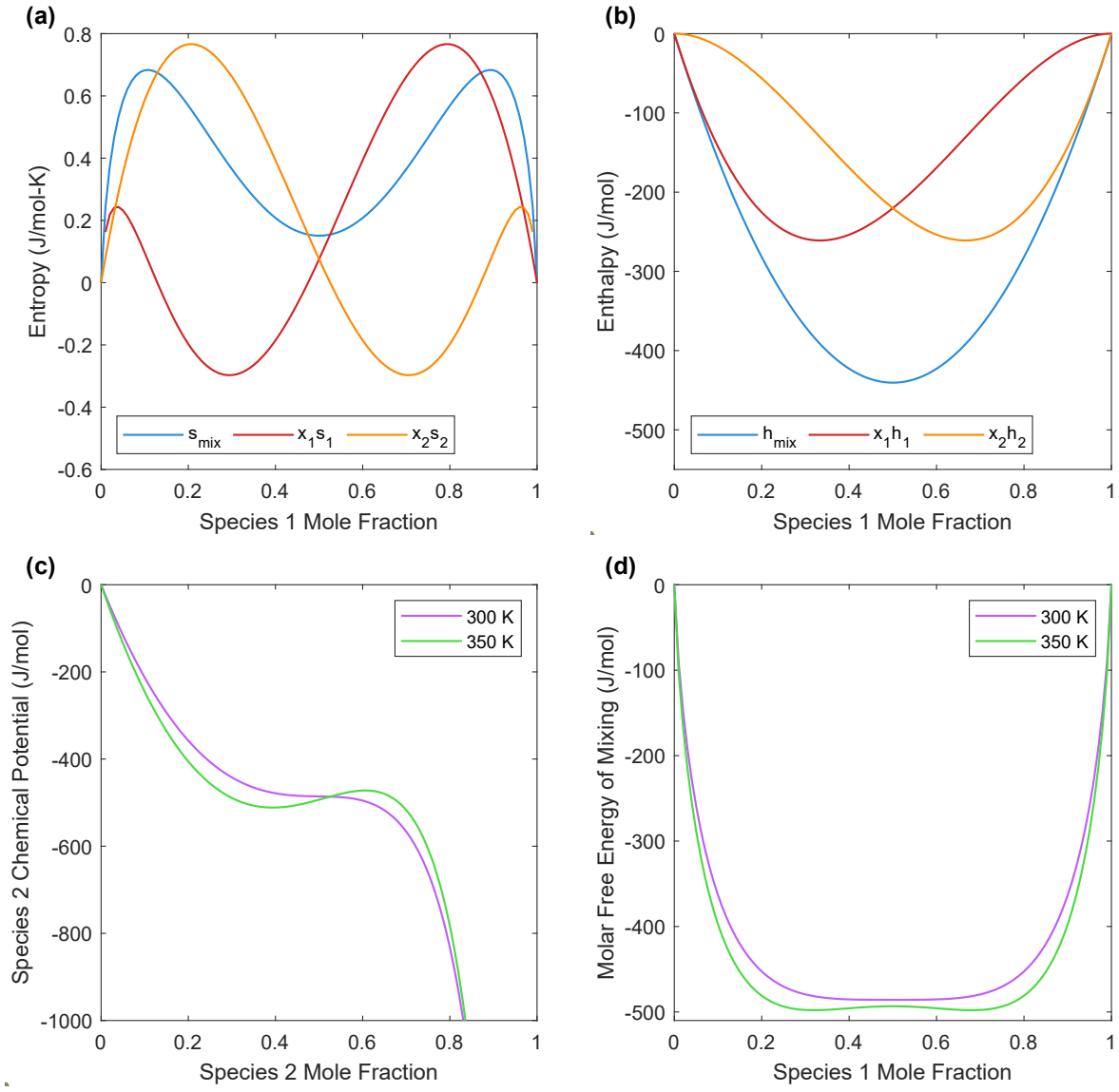

Fig. S5. LCST behavior in a modeled binary mixture with a positive entropy of mixing. (a) Entropy of mixing and partial molar entropies of both species. (b) Enthalpy of mixing and partial molar entropies of both species. (c) Chemical potential at a temperature below the LCST (300 K) and above the LCST (350 K). (d) Free energy of mixing at a temperature below the LCST (300 K) and above the LCST (350 K).

Supplementary Note 6: Endothermic Separation Proof

Because we show in the previous section that a positive entropy of mixing can lead to LCST phase behavior, it is important to also determine whether the separation of an LCST mixture is strictly endothermic, or if it could, in theory, be exothermic. Exothermic separation would involve a mixture that absorbs sensible heat as it is heated up to the LCST, but it would then begin releasing heat as its temperature is further raised above the LCST and separation occurs. In this section, we show that exothermic LCST separation is non-physical and such a mixture cannot exist. While this seems intuitive, we wanted to provide a rigorous proof of the fact. We show that both an LCST mixture with a negative entropy of mixing and an LCST mixture with a positive entropy of mixing would endothermically separate, which is described by the inequality in Eq. (S13).

$$Q_{sep} = \int T ds_{sep} > 0 \tag{S13}$$

To prove that all LCST mixtures must absorb heat upon separation (*i.e.*, endothermic separation), we first illustrate a T-S diagram of the non-physical exothermic separation in Fig. S6. This T-S diagram is essentially the reverse of the one in Fig. 4 of the main text. Instead of heat being absorbed during separation (process 2 – 3), heat is released. Then, the first and second laws of thermodynamics dictate that during mixing (process 4 – 1), work be done on the mixture as it absorbs heat. The need to do work to induce mixing would indicate that mixing is not spontaneous at T_1. However, because LCST mixtures are miscible in all proportions below the LCST, mixing must be spontaneous. Thus, the exothermic separation depicted in Fig. S6 is non-physical.

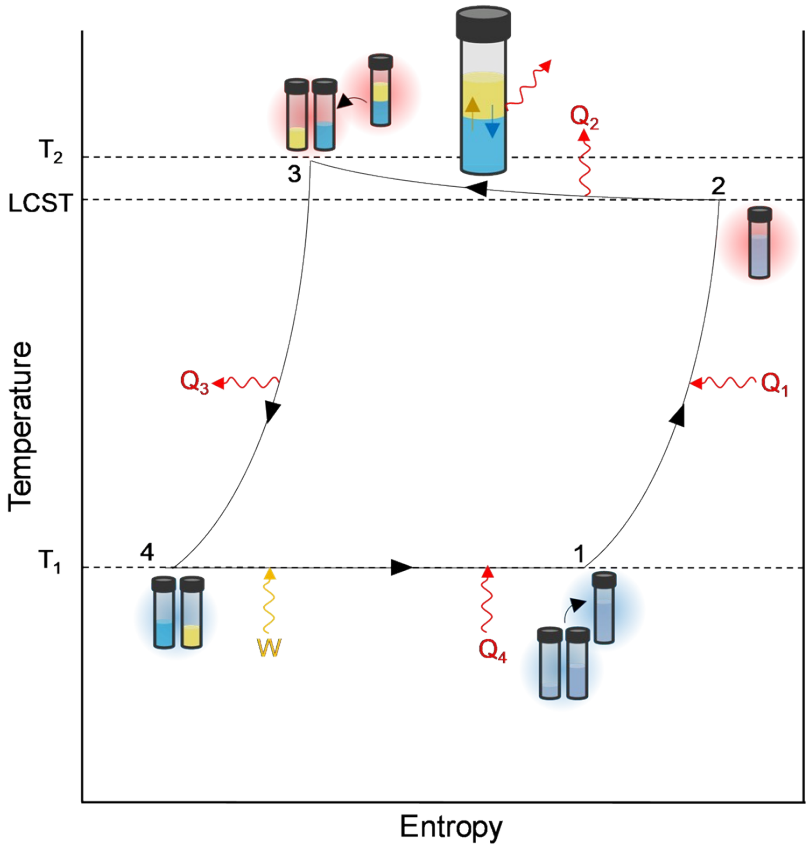

Fig. S6. T-S diagram of the cycling of a hypothetical LCST mixture that would release heat during separation; the T-S diagram indicates that this is impossible/non-physical.

To further illustrate that LCST separation must always be endothermic, we present the free energy of mixing of two different LCST mixtures in Fig. S7. Fig. S7a corresponds to a negative entropy of mixing, while Fig. S7b corresponds to a positive entropy of mixing. Turning first to Fig. S7a, we must establish that Eq. (S13) holds, which requires knowledge of the entropy of mixing, which can be determined from Eq. (S14).

$$\lim_{\Delta T \to 0} \left(\frac{\Delta g}{\Delta T} \right) = \frac{\partial g}{\partial T} = - s_{mix} \tag{S14}$$

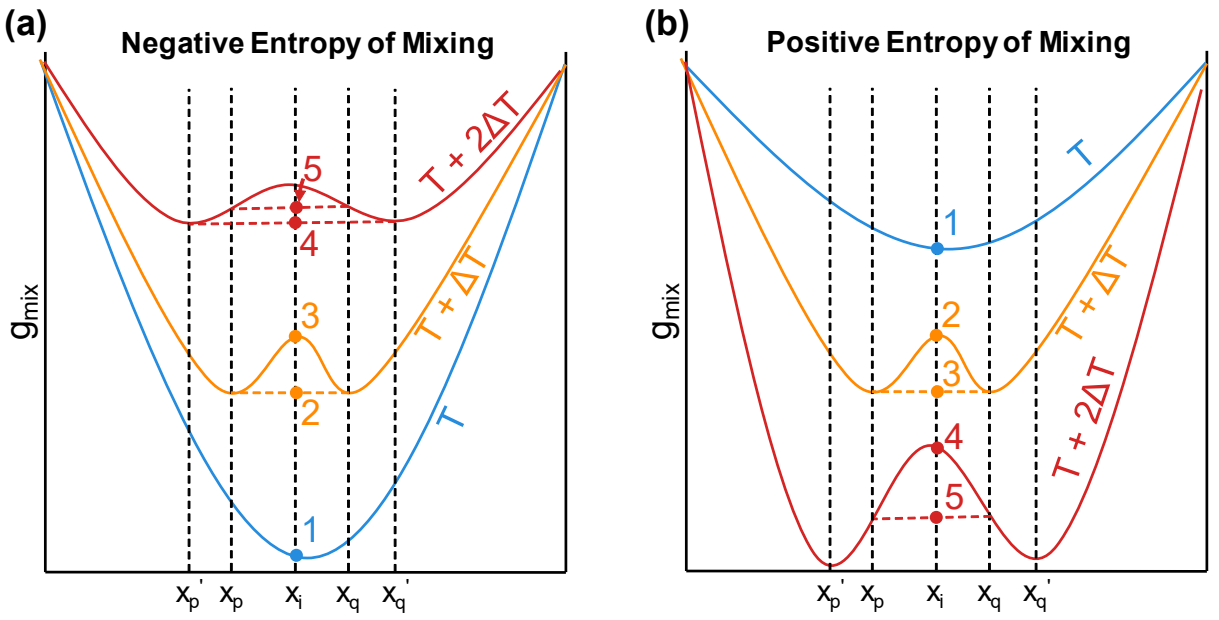

Fig. S7. (a) Free energy of mixing in an LCST mixture with a negative entropy of mixing. (b) Free energy of mixing in an LCST mixture with a positive entropy of mixing.

Initially at some temperature T (incrementally lower than the LCST) and concentration x_i, the mixture starts as homogenous (single-phase); this is labeled as state 1 in Fig. S7a. At this initial state, the free energy is g_1. Then, the mixture temperature is increased by an infinitesimal amount, ΔT, which is above the LCST. At this temperature, the free energy of mixing of the single-phase mixture is g_3, while the free energy of mixing of the two-phase mixture is g_2. Thus, for an incremental change in temperature ΔT, the change in free energy of the single-phase mixture (*SP*) is $\Delta g_{SP} = g_3 - g_1$, while the change in free energy of the two-phase mixture (*TP*) is $\Delta g_{TP} = g_2 - g_1$. Because the mixture spontaneously separates into the two-phase mixture, $\Delta g_{SP} > \Delta g_{TP}$. From Eq. (S14), this means that $s_{TP} > s_{SP}$, indicating the entropy is increasing upon separation, and heat is being absorbed. This holds even as the mixture continues to separate. When the mixture is heated further (from $T + \Delta T$ to $T + 2\Delta T$), the concentrations of the two phases go from x_p and x_q to x_p' and x_q'. At a temperature of $T + 2\Delta T$ f, the free energy of the two-phase

mixture at x_p and x_q is g_5, while the free energy of the two-phase mixture at $x_p^{'}$ and $x_q^{'}$ is g_4. Thus, upon increasing the temperature from $T + \Delta T$ to $T + 2\Delta T$, the change in free energy of the mixture at x_p and x_q is $\Delta g_{TP} = g_5 - g_2$, while the change in free energy of the mixture at $x_p^{'}$ and $x_q^{'}$ is $\Delta g_{TP'} = g_4 - g_2$. Because the new two-phase state (*TP'*) is more favorable than the old two-phase state at $T + 2\Delta T$, $\Delta g_{TP} > \Delta g_{TP'}$. From Eq. (S14), this again means that entropy is increasing upon separation. This holds for any temperature at which separation occurs, such that ds_{sep} is always positive, and the inequality in Eq. (S13) is always true.

We use this same procedure to establish that the entropy is also increasing upon separation for the system with the positive entropy of mixing in Fig. S7b. When heated from T to $T + \Delta T$, the change in free energy of the single-phase mixture is $\Delta g_{SP} = g_2 - g_1$, while the change in free energy of the two-phase mixture is $\Delta g_{TP} = g_3 - g_1$. Because the two-phase mixture is favorable, $|\Delta g_{SP}| < |\Delta g_{TP}|$ (*i.e.*, the free energy of the two-phase state decreases more than that of the single-phase state). However, since these changes are negative, it is clear that $\Delta g_{SP} > \Delta g_{TP}$, and therefore $s_{TP} > s_{SP}$. The same logic applies as heating continues, and entropy continues to increase upon separation. Thus, regardless of whether the mixture has a positive or negative entropy of mixing, all LCST mixtures will increase in entropy (and thus absorb heat) when they are heated to induce phase separation at temperatures above the LCST.

Supplementary Note 7: Enthalpy of Separation Derivation

The enthalpy of separation in Eq. (21) of the main text is simply equal to Q_{sep} (from Eq. (20)), normalized by the total number of moles of initial mixture: $\Delta h_{sep} = Q_{sep}/n$. In process 4 to 1 of the hypothetical cycle in Fig. 5b of the main text, water is transported from the WR phase to the WS phase, while the amount of IL (or, more broadly, all non-water species) in each phase remains constant. Then, n_w is the moles of water transported between the two phases, and w is the moles of water transported, normalized by the number of moles of initial mixture: $w = n_w/n$.

In the following analysis, it is necessary to find the range that w spans during process 4 to 1 in the cycle in Fig. 5b of the main text. The final value of w is that in which the WR and WS phases have both converged to the initial mixture concentration before separation, x_i. During the water transport process, the mole fraction of IL in the WR phase (x_A) is given in Eq. (S15), while the mole fraction of IL in the WS phase (x_B) is given in Eq. (S16).

$$x_A = \frac{n_{IL,WR}}{n_{WR,sep} - n_w} \tag{S15}$$

$$x_B = \frac{n_{IL,WS}}{n_{WS,sep} + n_w} \tag{S16}$$

In Eq. (S15), $n_{WR,sep}$ is the number of moles in the WR phase immediately following separation, which, using the lever rule, can be expressed as $n_{WR,sep} = n\frac{x_{WS} - x_i}{x_{WS} - x_{WR}}$. Likewise, $n_{WS,sep}$ is the number of moles in the WS phase immediately following separation, which can be expressed as

$n_{WS,sep} = n\frac{x_i - x_{WR}}{x_{WS} - x_{WR}}$. Furthermore, $n_{IL,WR}$ and $n_{IL,WS}$ are constant during process 4 to 1 (since only water is transported between the phases and not IL), so n_w is the only term that varies in Eq. (S15) and (S16) and is the mass transport coordinate for this process. Because x_A and x_B must be equal at state 1 (the end of the water transport process), Eq. (S17) results, which sets the two mole fractions equal when the full amount of water has been transported ($n_{w,f}$).

$$\frac{n\frac{x_{WS} - x_i}{x_{WS} - x_{WR}} - n_{w,f}}{n_{IL,WR}} = \frac{n\frac{x_i - x_{WR}}{x_{WS} - x_{WR}} + n_{w,f}}{n_{IL,WS}} \tag{S17}$$

Rearranging Eq. (S17) yields Eq. (S18), which can be further manipulated to produce Eq. (S19).

$$n_{w,f}\left(\frac{1}{n_{IL,WS}} + \frac{1}{n_{IL,WR}}\right) = n\left[\frac{x_{WS} - x_i}{n_{IL,WR}(x_{WS} - x_{WR})} - \frac{x_i - x_{WR}}{n_{IL,WS}(x_{WS} - x_{WR})}\right] \tag{S18}$$

$$\frac{n_{w,f}}{n} = \frac{\frac{x_{WS} - x_i}{n_{IL,WR}(x_{WS} - x_{WR})} - \frac{x_i - x_{WR}}{n_{IL,WS}(x_{WS} - x_{WR})}}{\frac{1}{n_{IL,WS}} + \frac{1}{n_{IL,WR}}} \tag{S19}$$

The quantity $n_{IL,WR}$ can be expressed as $n_{WR,sep}x_{WR}$, which can further be rewritten as $n_{IL,WR} = n\frac{x_{WS} - x_i}{x_{WS} - x_{WR}}x_{WR}$; likewise, $n_{IL,WS} = n\frac{x_i - x_{WR}}{x_{WS} - x_{WR}}x_{WS}$. Thus, Eq. (S19) can be rewritten

as Eq. (S20), which can be further simplified to Eq. (S21) by recognizing that $\frac{1}{x_{WR}} - \frac{1}{x_{WS}} = \frac{x_{WS} - x_{WR}}{x_{WR}x_{WS}}$

$$\frac{n_{w,f}}{n} = \frac{\frac{1}{x_{WR}} - \frac{1}{x_{WS}}}{\frac{x_{WS} - x_{WR}}{(x_{WS} - x_i)x_{WR}} + \frac{x_{WS} - x_{WR}}{(x_i - x_{WR})x_{WS}}} \tag{S20}$$

$$\frac{n_{w,f}}{n} = \frac{\frac{1}{x_{WR}x_{WS}}}{\frac{1}{(x_{WS} - x_i)x_{WR}} + \frac{1}{(x_i - x_{WR})x_{WS}}} \tag{S21}$$

Finally, Eq. (S21) can be rewritten as Eq. (S22).

$$\frac{n_{w,f}}{n} = \frac{1}{\frac{x_{WS}}{(x_{WS} - x_i)} + \frac{x_{WR}}{(x_i - x_{WR})}} \tag{S22}$$

Thus, w spans a range of 0 (*i.e.*, the beginning of the process when no water has been transported) to $\left(\frac{x_{WS}}{x_{WS} - x_i} + \frac{x_{WR}}{x_i - x_{WR}}\right)^{-1}$ (*i.e.*, the value that causes the WR and WS phases to have the same concentration), where x_i is the mole fraction of IL in the initial mixture before separation, state 1 (which is the same as the mole fraction of the IL at the end of the water transport process 4 to 1).

By integrating Eq. (19) of the main text, it is clear that the work produced by this hypothetical cycle is $W = \int_0^{n_{w,f}} \Delta\mu_w dn_w$, where $\Delta\mu_w$ is the chemical potential of water difference between the two phases at ambient temperature (T_1): $\Delta\mu_w = \mu_w(x_A, T_1) - \mu_w(x_B, T_1)$, where x_A is the concentration of the WR phase throughout process 4 to 1, and x_B is the concentration of the WS phase throughout the process. As water is shared, the chemical potential difference will decrease, so $\Delta\mu_w$ is a function of n_w. Rewriting the integral above in terms of the dimensionless quantity w yields $\frac{W}{n} = \int_0^{\left(\frac{x_{WS}}{x_{WS}-x_i} + \frac{x_{WR}}{x_i - x_{WR}}\right)-1} \Delta\mu_w dw$. From Eq. 19 of the main text, the following relationship for the enthalpy of separation results: $\Delta h_{sep} = \frac{Q}{n} = \frac{W}{n}\left(1 - \frac{T_{amb}}{T_{sep}}\right)^{-1}$, which can be rewritten in the form in Eq. (S23).

$$\Delta h_{sep} = \frac{\int_0^{\left(\frac{x_{WS}}{x_{WS}-x_i} + \frac{x_{WR}}{x_i - x_{WR}}\right)-1} \Delta\mu_w dw}{1 - T_{amb}/T_{sep}} \tag{S23}$$

Furthermore, the integral term in Eq. (S23) can be expressed as an average chemical potential difference, which is given in Eq. (S24). From Eq. (S23) and (S24), Eq. (21) and (22) of the main text result.

$$\Delta\tilde{\mu}_w = \frac{1}{\left(\frac{x_{WS}}{x_{WS}-x_i}+\frac{x_{WR}}{x_i-x_{WR}}\right)^{-1}} \int_0^{\left(\frac{x_{WS}}{x_{WS}-x_i}+\frac{x_{WR}}{x_i-x_{WR}}\right)^{-1}} \Delta\mu_w dw \quad \text{(S24)}$$

References

1. Haddad, A. Z. *et al.* Solar Desalination Using Thermally Responsive Ionic Liquids Regenerated with a Photonic Heater. *Environ. Sci. Technol.* **55**, 3260–3269 (2021).
2. Kohno, Y. & Ohno, H. Temperature-responsive ionic liquid/water interfaces: relation between hydrophilicity of ions and dynamic phase change. *Phys. Chem. Chem. Phys.* **14**, 5063–5070 (2012).
3. Kamio, E., Takenaka, A., Takahashi, T. & Matsuyama, H. Fundamental investigation of osmolality, thermo-responsive phase diagram, and water-drawing ability of ionic-liquid-based draw solution for forward osmosis membrane process. *Journal of Membrane Science* **570–571**, 93–102 (2019).
4. Longeras, O., Gautier, A., Ballerat-Busserolles, K. & Andanson, J.-M. Deep Eutectic Solvent with Thermo-Switchable Hydrophobicity. *ACS Sustainable Chem. Eng.* **8**, 12516–12520 (2020).
5. Kocher, J. D., Menon, A. K. & Yee, S. K. An Air Conditioning Cycle Using Lower Critical Solution Temperature Mixtures. in (American Society of Mechanical Engineers Digital Collection, 2023). doi:10.1115/HT2023-107065.
6. Mahfouz, A. N., Haddad, A. Z., Kocher, J. D. & Menon, A. K. Performance enhancement of aqueous ionic liquids with lower critical solution temperature (LCST) behavior through ternary mixtures. *J. Mater. Chem. A* (2024) doi:10.1039/D4TA07575G.
7. Schroeder, D. V. *An Introduction to Thermal Physics*. (Oxford University Press, 2021).
8. Moran, M. J., Shapiro, H. N., Boettner, D. D. & Bailey, M. B. *Fundamentals of Engineering Thermodynamics*. (John Wiley & Sons, 2010).